Physica B 649 (2023) 414470

Contents lists available at ScienceDirect

Physica B: Condensed Matter

journal homepage: www.elsevier.com/locate/physb

Insight into the electronic structure, magnetic, and thermoelectric properties of transition metal pnictides KCr_2L_2 (K= Ca, Sr; L = P, As): As substitute source for renewing energy

Zeshan Zada [a], Abdul Ahad Khan [b], Ali H. Reshak [c,d,e,*], Irfan khan [f], Shafqat Zada [g], Muhammad Ismail [h], Muhammad Fazal-ur-Rehman [i], Muhammad Saqib [j], G. Murtaza [k], Qaisar Khan [l], Muhammad M. Ramli [d]

[a] Beijing National Laboratory for Condensed Matter Physics, Institute of Physics, Chinese Academy of Sciences, Beijing, 100190, China
[b] Department of Physics, University of Peshawar, Peshawar, 25120, Pakistan
[c] Physics Department, College of Science, University of Basrah, Basrah, 61004, Iraq
[d] Center of Excellence Geopolymer and Green Technology (CEGeoGTech), University Malaysia Perlis, 01007, Kangar, Perlis, Malaysia
[e] Department of Instrumentation and Control Engineering, Faculty of Mechanical Engineering, CTU in Prague, Technicka 4, 616607, Prague, Czech Republic
[f] Department of Physics, University of Sargodha, Sargodha, Punjab, Pakistan
[g] Department of BioChemistry, Quaid Azam University of, Islamabad, Pakistan
[h] Department of Chemistry, Women Univeristy Swabi, KP, Pakistan
[i] Chemistry Department, University of Education Lahore, Vehari Campus, Vehari, Punjab, Pakistan
[j] Department of Electrical and Computer Engineering, COMSATS University Islamabad, Abbottabad Campus, Abbottabad, 22060, Pakistan
[k] Materials Modeling Lab, Department of Physics, Islamia College University, Peshawar, 25120, Pakistan
[l] Department of Physical and Biological Sciences, Islamia College Peshawar, Peshawar, 25120, Khyber Pakhtunkhwa, Pakistan

ARTICLE INFO

Keywords:
Thermoelectric properties
Magnetic
Transition metal pnictides
Renewing energy
Antiferromagnetic
First-principles

ABSTRACT

In this study, we have investigated the electronic structure, magnetic and thermoelectric properties of the antiferromagnetic (A-AFM) phase for ternary KCr_2L_2 (K= Ca, Sr; L = P, As) compounds using the framework of full-potential augmented plane wave method within the generalized gradient (PBE-GGA) approximations. We determined that the presence of the A-AFM phase is more favorable among the possible spin phases at their relaxed lattice parameters. Based on the stable phase, we found that both Cr atoms are well modulated in AFM phase. Furthermore, we have investigated the thermoelectric properties for all investigated compounds from 50 K to 800 K. Our calculations suggest the $SrCr_2As_2$ and $SrCr_2P_2$ compound can obtain high figure of merit values ~1 with optimized carrier concentration at lower temperature, indicating the strontium based compounds are promising candidate for low-temperature thermoelectric device. In all, our calculations discover the novel ternary KCr_2L_2 (K= Ca, Sr; L = P, As) compounds with promising physical properties for potential spintronics and magnetic application.

1. Introduction

The exploration for novel functional materials with excellent properties for modern industrial and technological applications has motivated the theoretical researchers in material community to predict and pre-select the candidates of functional materials. A colossal increase in simulation power and the algorithmic improvements in quantum theory permit one to have efficient and accurate estimations of material properties [1,2]. The last decade has witnessed significant development in ab-initio calculations including the expansion flavors like GGA + U, mBJ [3–5]. These flavors has broadened the extent of ab-initio calculation and the calculated results are much closer to experimental and theoretical results.

Since last few years, the layered transition metal compounds have displayed their intriguing physical properties, e.g., high magnetoresistance [11], magnetisms, superconductivity [6–9], and charge density waves (CDWs) [10]. The surprising discovery of superconductivity in layered iron-based compounds [12–14] has made an incredible shock to

* Corresponding author. Physics Department, College of Science, University of Basrah, Basrah, 61004, Iraq.
E-mail address: maalidph@yahoo.co.uk (A.H. Reshak).

https://doi.org/10.1016/j.physb.2022.414470
Received 18 August 2022; Received in revised form 19 October 2022; Accepted 30 October 2022
Available online 5 November 2022

the whole high-temperature (high-Tc) superconductivity research community. From then on, iron-based superconductors have been one of the most popular research fields in condensed-matter physics and further attracted research attention on the corresponding layered pnictides. These promising materials show large potential in colossal" or "giant" magneto-resistive (CMR or GMR) applications such as magnetic field sensors, spin filters, and spin valves [15–18]. The GMR can also be utilized latest innovative devices such as micro-electromechanical systems (MEMS), hard disk drives and biosensors Interestingly, the Zintl phases with numerous structures have also been considerably investigated for their attractive magnetic properties, significant for application in magnetic read heads [19] and single molecule magnets [20].

Zintl compounds have a strong history of scientific study since their early discovery from Edward Zintl in the 1930s [21–23]. Currently, these compounds regain the interest of scientist due to their intriguing electronic, optical, elastic, and thermoelectric properties [24,25]. A thorough investigation of electro-positively charged compounds of the type AB_2X_2 (A = Ba/Sr/Ca; B = Zn, Cd; X = Sb/As/P) has been reported, demonstrating that these compounds crystallize in the novel trigonal ($CaAl_2Si_2$) structure with B element in a spherically symmetric distribution of d-electron (d^0, d^5 and d [10] configuration). The radius ratio (r_a: r_b) of A and B site element is a key factor for the formability AB_2X_2 structure, whereas the size of the X element has negligible effect. The KCr_2L_2 compound adopts the trigonal $CaAl_2Si_2$-type structure with space group P 3 m1 (No. 164) [26]. By comparing the tetragonal and hexagonal 122 families of pnictides for the search of magnetic properties, the author's noted that the overall nature of magnetism in both structure are quite similar by replacing transition metal, which is due to the presence of iron-based high-temperature superconductors in the structure [26]. In the 122 tetragonal family, the A site has an extremely limited effect on electronic as well as magnetic structure. In the two families, the next-nearest-neighbor (NNN) effective antiferromagnetic (AFM) exchange couplings reach the maximum peak value in the iron-based materials.

With the assistance of neutron scattering, it has been realized that isostructural $BaMn_2Bi_2$ owns the same G-type AFM structure as $BaMn_2As_2$ and has a lower T_N = 387 K [27]. Especially, $ThCr_2Si_2$ and $CaAl_2Si_2$ structure are mostly studied [28–33].

In order to know more about the type of electronic configurations, Zheng and Hoffmann worked on these calculations show little significance of the A cation, while shed light on the bonding nature within the $B_2X_2^{2-}$ layers. In a special case, Zheng and Hoffmann performed study on AMn_2P_2 compounds [31]. Either $CaAl_2Si_2$ structure type is obtained from this composition (A = Sr, Ca) [34] or $ThCr_2Si_2$ structure type (A = Ba) [35].

Moreover, materials with incredible TE characteristics are of astonishing attention since great TE materials can be used as a substitute source for renewing large amount of wasting heat from vehicles and mega factories [36]. Devices subject to these materials and can be utilized to generate electricity by changing waste heat [37]. This procedure is exceptionally encouraging for the recovery of waste heat and for tending to worldwide environmental issues. The immediate change of heat energy to electricity, and the thermoelectric effect is a topic that material physics has long been interested in [38]. We need to look at the thermoelectric parameters and the component involved to overall upgrade the TE properties of materials.

However, to the best of our knowledge, no attention has been paid to the theoretical simulations of thermoelectric properties of these compounds. In the present work, first principle calculation based on Density function theory will be implemented to investigate different physical properties most notably, electronic, magnetic and thermoelectric properties.

2. Computation details

The present calculation was carried out using the full potential augmented plane wave (FPAPW) method based on the density functional theory [39,40] with the implementation of the WIEN2k code [41]. We used the approximation parameterized by the Perdew-Burke-Ernzerhof (PBE-GGA) [42] and GGA plus Hubbard (GGA + U) scheme for the (exchange correlation) energy. The plane wave cutoff parameter of R*K*max was set as 7.0/RMT (where R is the average radius of muffin-tin spheres and the reciprocal lattice constant Kmax is the highest value that can be utilized in plane wave expansion. This approach is based on the partitioning of the entire crystal into non-overlapping muffin-tin (Mu-T) spheres separated by an interstitial area. A simple basis set function is chosen and further expanded at this point in favor of spherical harmonic functions within MT spheres, and simple plane waves are also used in the interstitial area. The biggest vector (Gmax) in the Fourier expansion of the charge density has a magnitude of 12 atom unit $(au)^{-1}$ [7,9,47,49]. We choose 0.0001Ry for energy convergence and 0.001e for charge convergence in the self-consistency cycle. Further we did not account for the effect of spin orbit coupling in our calculations. The separation energy between valence and core states is −6.0 Ry. For the elements (Ca, Cr, P), (Ca, Cr, As), (Sr, Cr, P), and (Sr, Cr, As), respectively, we used the values of non-overlapping muffin-tin radii (M-T-R) as (2.5, 2.02,1.74), (2.3, 2.1, 2.0), (2.0, 2.0, 2.0), and (2.0, 2.0, 2.0) a. u. We have purposed 1000 *k* points Monkhorst–Pack mesh [43,44] in the Brillion zone for $CaCr_2P_2$, $CaCr_2As_2$, $SrCr_2P_2$ and $SrCr_2As_2$ compounds in the AFM phase.

3. Results and discussion

3.1. Structural properties

The optimization processes are performed in five phases, different structures: non-magnetic (NM), ferromagnetic (FM) and three antiferromagnetic, AFM I (A-type), AFM II (C-type) and AFM III (G-type) structures respectively as shown in Fig. 1 and Table 1 [47,48,53]. We find an increment in the lattice constant (*a*) and volume (V_0) on replacing the cations or anions due to the difference in atomic size and electronegativity. Furthermore, the energy calculated results show the studied materials stabilize in the AFM I configuration, which was recently reported by other researcher for the same family of other compounds [47,48]. our computed structural properties match the other theoretical reports [6] quite well (see Fig. 1).

3.2. Electronic properties

In electronic properties, we have calculated the total spin density of states (TDOS) and partial density of states (PDOS) in AFM phase as shown in Fig. 2. The total and projected density of states (DOS) help us to know the contribution of different states in conduction and valence bands. The dominant contributions for $CaCr_2P_2$ and $CaCr_2As_2$ come from *d* (Ca, Cr_1, Cr_2), *p* (P) and *d* (Ca, Cr_1, Cr_2), *p* (As) states, respectively. In spin-up and spin-down channels both *d* states of Cr atoms contribute oppositely, it means that both Cr atoms are well adjusted antiferromagnetically. The peaks near the E_f are from *d* (Cr) states while far from the E_f come from *p* (P, As) states., point out hybridization of these elements to Cr element respectively. Due to the double exchange, the hybridization mechanism is important for AFM's partial d-band filling. The AFM states show direct exchange couplings between two nearest-neighbors (NN) of Cr atoms [6]. The conduction and valence bands are mixed at the Fermi level in both compounds, howing the metallic behavior of the AFM phase in both up and down spin types.

For $SrCr_2P_2$ and $SrCr_2As_2$ the designed plots of DOS are shown in schematic Fig. 3. The *d* (Sr, Cr_1, Cr_2), *p* (P), *d* (Sr, Cr_1, Cr_2) and *p* (As) states contribute majorly in $SrCr_2P_2$ and $SrCr_2As_2$ in both spin channels. The foremost role of (Sr) Cation and (P, As) anions states are appearing predominantly in both spin channels and located in CB/VB. The dominant contribution of (Cr) *d* states spans over a larger range across the E_F which play a significant role in conductivity of these compounds. The

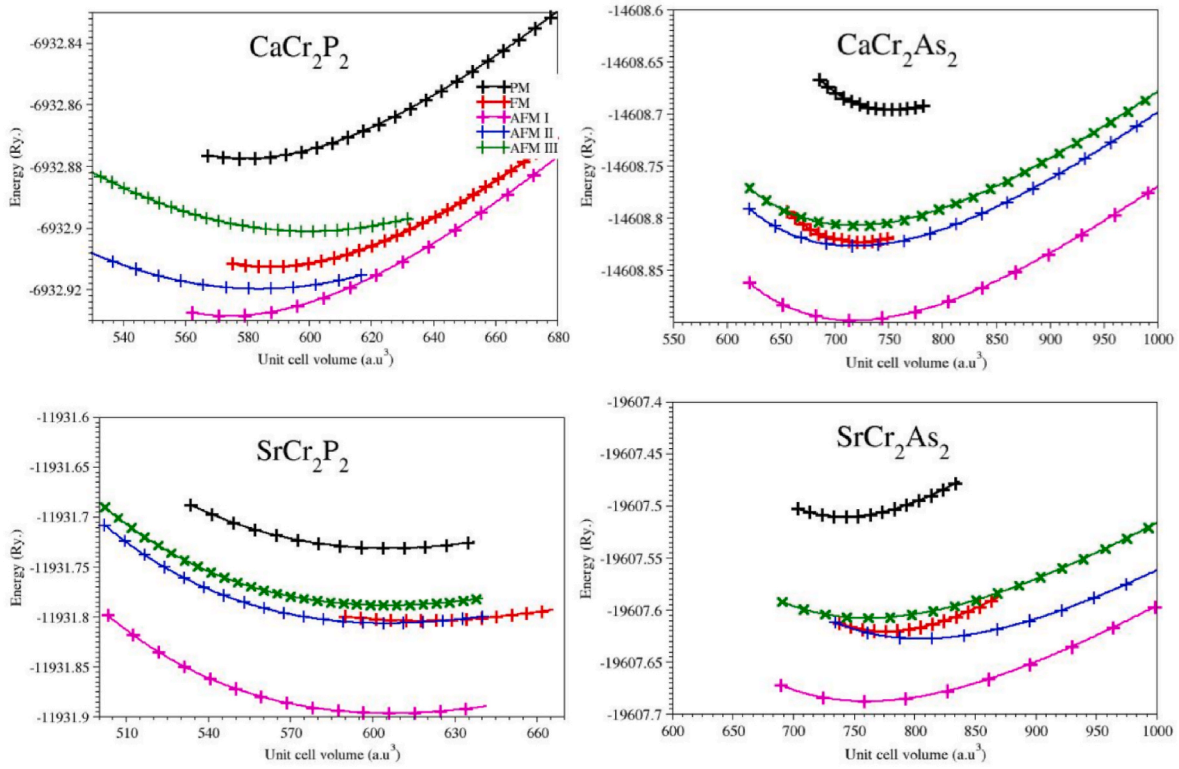

Fig. 1. Optimization plots for $CaCr_2P_2$, $CaCr_2As_2$, $SrCr_2P_2$ and $SrCr_2As_2$ displaying energy verses volume.

Table 1
Calculated antiferromagnetic ternary compound lattice parameters, including *a* (Å), B (GPa), Bp and E_0 (Ry), as well as other theoretical findings.

Compound	Lattice constant (Å)		V_0 (a.u) [3]	B(GPa)	B_p	E_0 (Ry)		
	a	c				A-AFM	C- AFM	G-AFM
$CaCr_2P_2$	3.96	6.98	574.99	122.69	4.04	−6932.96	−6932.92	−6932.90
Exp.	–	–						
Other Calc.	3.97[(a)]	7.02[(a)]						
$CaCr_2As_2$	4.1	7.33	717.40	63.73	5.21	−14608.89	−14608.84	−14608.81
Exp.	–	–						
Other Calc.	4.1[(a)]	7.27[(a)]						
$SrCr_2P_2$	4.01	7.21	605.55	110.91	5.00	−11931.9	−11931.81	−11931.79
Exp.	–	–						
Other Calc.	–	–						
$SrCr_2As_2$	4.17	7.63	764.39	69.61	6.58	−19607.69	−19607.64	−19607.61
Exp.	–	–						
Other Calc.	–	–						

[a] Ref [6].

beginning and closing of Cr_1-d and Cr_2-d states are accurately analogous to one another in the understudy compounds as essential for an AFM. Moreover, it shows most prominent result that both Cr atoms in AFM phase are well coupled antiferromagnetically. In both the compounds, *p-d* coupling gives evidence of hybridization dominantly between *p* (p, As) and *d* (Cr) states respectively. The DOS of the both compounds show metallic character across the Fermi level in both up and down spin states.

Moreover, along the stable AFM phase, we have also worked out on PM phase due to the fact that it may exist in the PM phase above the Néel temperature. From projected DOS, as shown in Fig. 4, one can see that *d* (Ca, Sr, Cr) states and *p* (P, As) states have remarkably contributed to the DOS, in the PM phase. The DOS near the Fermi level of PM phase suggest the metallic nature of our studied materials and may be unstable based on the Stoner argument [45], and another possible phase (lower-energy structure) is easily achieved by allowing spin polarization or structural distortion.

3.3. Magnetic properties

To have a deeper comprehensive understanding and knowledgeable data about magnetic moment formation, we work out the local moments and the magnetic interaction in the KCr_2L_2. Here we have utilized GGA + *U* scheme, especially for the purpose to further enhance the localization of the element of transition metals (Cr) [49–51]. According to the DOS calculations, the magnetic moment of the chromium (Cr) atom has a greater influence than that of other atoms in both spin up and down types. The partially filled sub-*d* states are the primary source of magnetism. The magnetic moment's encouragingly positive result indicates that these compounds' magnetic ground states exhibit highly ferromagnetic activity. The over-all unit-cell magnetic moments are primarily composed of (K= Ca, Sr; L = P, As) atoms with minor contributions in aspect of Ca/Sr as well as interstitial site. In the compound KCr_2L_2, the Cr atom has a larger magnetic moment than the other atoms involved. Consequently, from the thorough investigation, we have noted

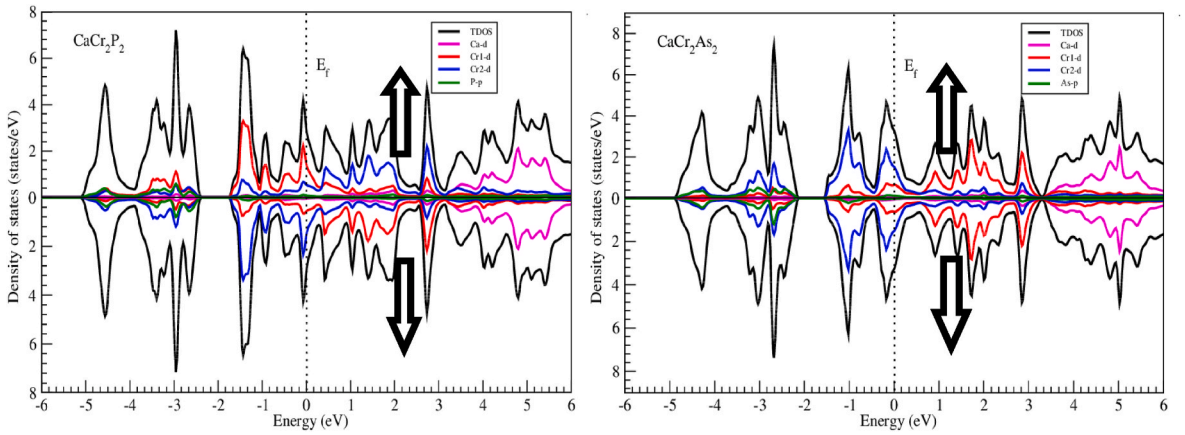

Fig. 2. The DOS plots for $CaCr_2P_2$ and $CaCr_2As_2$ in both spin up and down directions.

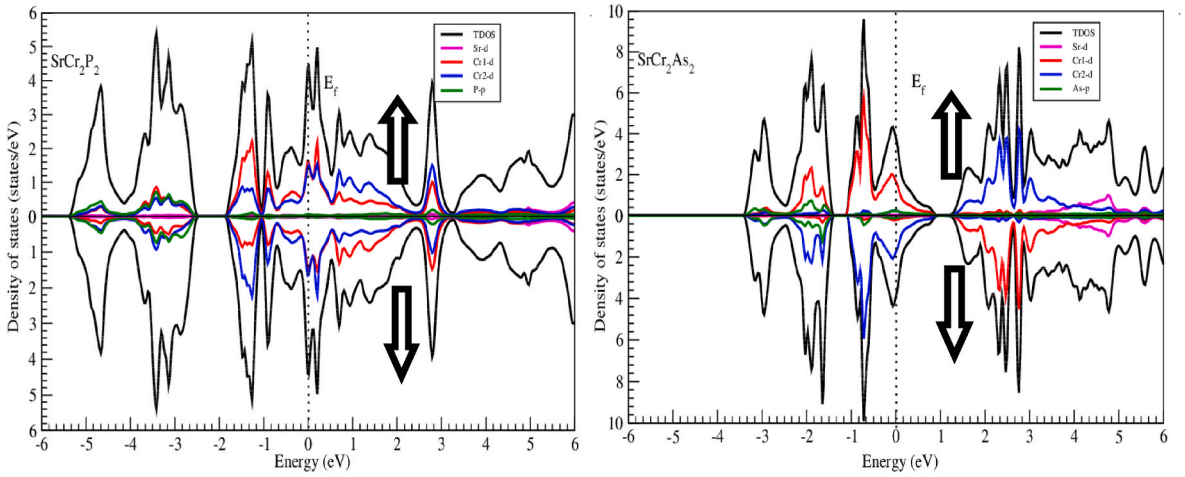

Fig. 3. The DOS plots for $SrCr_2P_2$ and $SrCr_2As_2$ in both spin configurations.

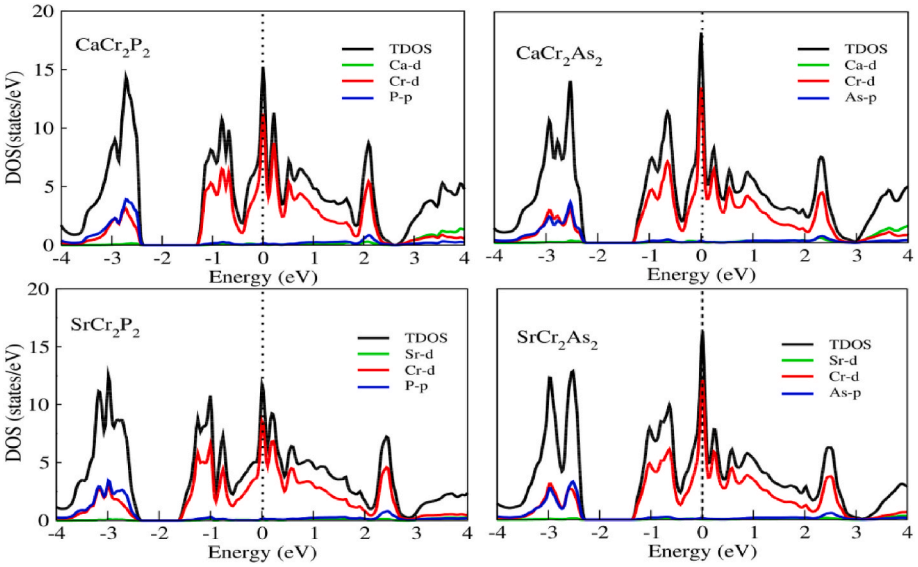

Fig. 4. DOS plots for paramagnetic ternary compounds.

that the magnetic moment of the Cr atom is greater than that of the Ca/Sr atoms. This is primarily because, according to the DOS calculations, the d-state of the Cr atoms appears free dominantly over the entire energy range in both spin up and down types. Furthermore, the negative minimum values of magnetic moment express the reliable signal of P/As atoms at all known locations in the unit-cell standing anti-parallel to the

complete ferromagnetic direction. The $\mathbf{m^c}$ (total cell magnetic moment) of all compounds, in addition to their (individual atomic and interstitial) magnetic moments, are also listed in Table 2.

3.4. Thermoelectric properties

Thermoelectric properties of investigated materials are calculated by semi classical theory using Boltztrap code [52–57]. Thermoelectric materials, directly converting low-grade waste heat into electricity, are promising in alleviating energy crisis and pollution. The conversion efficiency of thermoelectric devices mainly depends upon the material response, in particular the dimensionless figure of merits ZT expressed in the noted equation $ZT = S^2\rho^{-1}\kappa^{-1}T$, where T (absolute temperature), S (Seebeck coefficient), ρ and κ are electrical/thermal conductivity, respectively. The larger ZT value of material, the higher the conversion efficiency [52,53]. The high values of Seebeck coefficient and electrical conductivity with lower thermal conductivity is beneficial for high thermoelectric performance.

The electrical conductivity is a key parameter for the effectiveness of material. The electrical conductivity tensor can be written as

$$\sigma_{\alpha,\beta} = e^2\sum_{i,k}\left[\frac{-\partial f_o(T,\varepsilon,\mu)}{\partial\varepsilon}\right]v_\alpha v_\beta \mathrm{T}_k$$

Where $v_\alpha, v_\beta, \mathrm{T}_k$, denotes group velocities and relaxation time, (α, β) tensor indices, (μ) chemical potential and (f_o)Fermi Dirac distribution function.

The flow of free charge carriers, which can be observed in Figs. 2–4 band structure and density of states, is what causes electrical conductivity. Fig. 5 illustrates how excited electrons contribute to electrical conduction [57,59]. Whenever the temperature rises, strontium-based materials $SrCr_2As_2$ and $SrCr_2P_2$ show little increment in the electrical conductivity and doesn't change at high temperatures and stays zero. While the calcium-based compounds $CaCr_2As_2$ and $CaCr_2P_2$ exhibits gradual increase in electrical conductivity over the entire temperature range and reached their peak values at about 800 K. Further, the $CaCr_2P_2$ compound exhibit maximum electrical conductivity in comparison to other understudy compounds.

The electrical conductivity (σ) curve, which displays maximum values for calcium-based compounds, shows smaller values at the same temperature of roughly 50 K than the electronic thermal conductivity (κ/τ) curve. Therefore, the opposing trend is shown by both curves from their starting points. At higher temperature electrons achieve more thermal energy and start their movement from high temperature towards low temperature region in a thermoelectric device.

The thermal conductivity, which is dependent on free electrons and lattice vibrations, is the second crucial parameter. In case of semiconductors and metals, heat is transported produced due to lattice vibrations and charge-free carriers. The material should have low thermal conductivity for better thermoelectric performance [53]. Fig. 6 indicates that strontium based $SrCr_2As_2$ and $SrCr_2P_2$ compounds depict linear curves of electronic thermal conductivity (κ/τ) with temperature at about 400K and further increase in a temperature show little increase in thermal conductivity. The calcium based $CaCr_2As_2$ and $CaCr_2P_2$ compounds show linear relationship with temperature and gained its

Table 2
Magnetic moments (MM) of the interstitial region (m^{intst}), individual atoms ($m^{Ca/Sr/Cr/P/As}$) and total cell for KCr_2L_2 (K= Ca, Sr; L = P, As) for spin ferro configurations.

Compound	m^{intst}	$m^{Ca/Sr}$	m^{Cr}	$m^{P/As}$	m^c
$CaCr_2P_2$	0.76493	0.01288	3.71600	−0.19584	4.29797
$CaCr_2As_2$	0.80790	0.01949	3.72383	−0.14158	4.40964
$SrCr_2P_2$	0.66248	0.00327	3.61060	−0.19275	4.08359
$SrCr_2As_2$	0.84338	0.00758	3.73999	−0.13807	4.45287

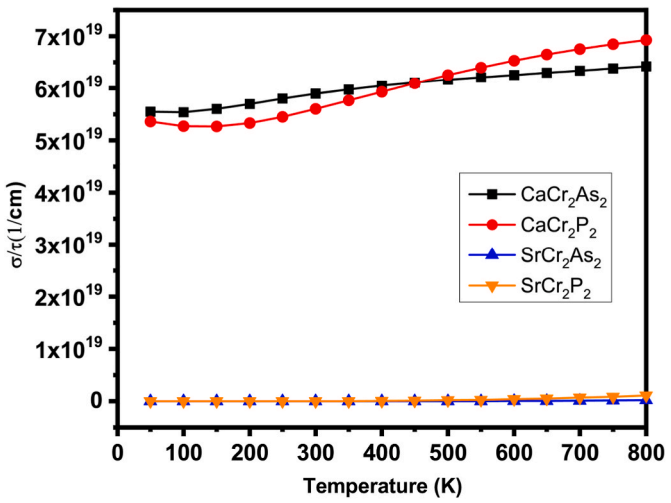

Fig. 5. Temperature-dependent variations in electrical conductivity (σ/τ) for KCr_2L_2 (K═Ca, Sr and L = As, P).

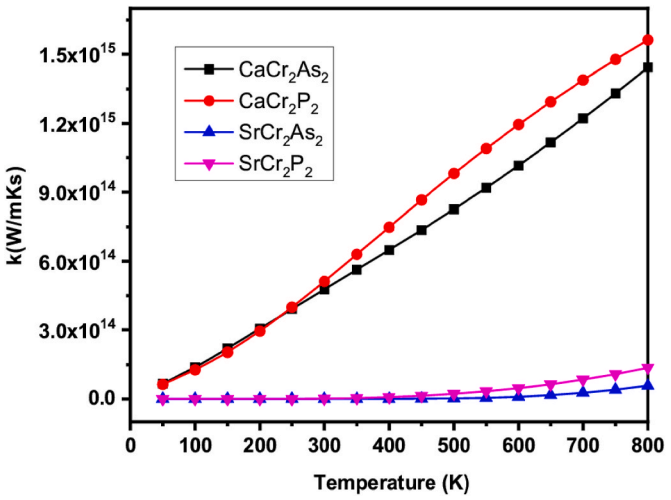

Fig. 6. Temperature-dependent variations in electronic thermal conductivity (κ/τ) for KCr_2L_2 (K═Ca, Sr and L = As, P).

maximum value at 800 K. This trend resembles that of electrical conductivity (σ) plots (Fig. 5). The same profile of both electrical and thermal conductivity curves is according to the Wiedemann-Franz law, it states that the relationship between the heat contribution and electrical conductivity is direct [46]. Furthermore, $CaCr_2P_2$ compound show maximum while $SrCr_2As_2$ compound indicate minimum value of electronic thermal conductivity (κ/τ) as compared to other compounds.

When two metal are at different temperatures, then electrons flow from the hot to the cold region, this effect is called Seebeck effect. Fig. 7 depicts the calculated Seebeck coefficient at a given temperature. It is indicated that all the four compounds show an increasing trend in the Seebeck coefficient S curve, with temperature and reach at their maximum values at about 100 K for $SrCr_2As_2$ and about 180 K for $CaCr_2P_2$, $CaCr_2As_2$ and $SrCr_2P_2$ compounds, respectively. The Seebeck coefficient (S) shows positive values for $CaCr_2As_2$ and $SrCr_2As_2$ over the entire temperature range, exhibiting compounds with p-type nature, while positive values till 350 K for $CaCr_2P_2$ and $SrCr_2P_2$ along with negative obtained values further higher in temperature ranges exhibit mix p-n type conduction behavior. When the temperature is raised further, a significant decrease in (S) is observed in almost all of the compounds across the entire temperature range. The maximum values attained by KCr_2L_2 zintl compounds are tabulated in Table 3.

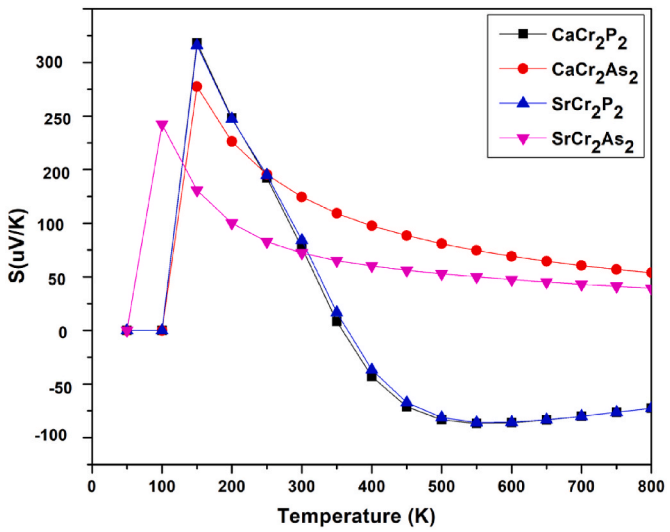

Fig. 7. Variation of Seebeck coefficient with temperature for KCr_2L_2 (K═Ca, Sr and L = As, P).

Table 3
Thermoelectric parameters (Seebeck coefficient, Thermal conductivities, Electrical conductivities, Power factor and ZT) for ternary compounds KCr_2L_2 (K= Ca, Sr; L = P, As).

Compounds	Seebeck coefficient (μV/K)	Thermal conductivities (W/Kms)	Electrical conductivities (1/cm)	Power factor (W/mK^{2}s)	ZT
$SrCr_2P_2$	323	1.4×10^{15}	6×10^{19}	5.0×10^{10}	0.1
$SrCr_2As_2$	248	1.6×10^{15}	7×10^{19}	1.0×10^{11}	0.09
$CaCr_2As_2$	275	0.2×10^{14}	0.001×10^{13}	4.0×10^{10}	0.8
$CaCr_2P_2$	324	0.4×10^{14}	0.0015×10^{13}	$1.25.0 \times 10^{11}$	0.6

Fig. 8 displays the calculated power factor (P.F.) for each compound under investigation. The P.F curve for calcium-based compounds $CaCr_2As_2$ and $CaCr_2P_2$ increases up to T = 330 K. Whereas the (P.F) curve for strontium-based compounds $SrCr_2As_2$ and $SrCr_2P_2$ remains low till 200 K, whereas further increase in temperature show linear increase in PF for both the compounds. Therefore, all of these compounds exhibit variations at high temperatures. Furthermore, the compound $CaCr_2P_2$ reached higher P.F value of about 350 K and decreased gradually in higher temperature. At 800 K, $SrCr_2P_2$ shows maximum PF of magnitude.

Figure of merit is parameter key index for evaluating the performance of thermoelectric materials. The material which a high (ZT) is considered to be more efficient as compared to low ZT [52,53,57–59]. It is clearly seen from Fig. 9 that the ZT values for strontium-based compounds $SrCr_2As_2$ and $SrCr_2P_2$ peaks higher than the other calcium-based compounds. The calculated maximum values for KCr_2L_2 (K═Ca, Sr and L = As, P) are provided in Table 3. These compounds have high ZT values in the low temperature region, making them excellent candidates for low temperature waste heat management applications. Further the ZT curve declines dramatically as the temperature rises for both the compounds. The ZT curves of calcium-based compounds possess a small ZT value (00 for $CaCr_2P_2$ and 00 for $CaCr_2As_2$) and show small variation. Overall, the strontium-based materials are promising candidates for thermoelectric devices.

Fig. 10 displays the calculated Temperature-dependent Carrier Concentration for each compound under investigation. The Carrier Concentration curve for KCr_2L_2 compounds increases over the entire temperature. Furthermore, the compound $SrCr_2P_2$ increased gradually at lower temperature (below 300 K) and the spectra achieved a higher Carrier Concentration value with a magnitude at about 800 K, the same as PF in (Fig. 8). All the compounds show a maximum value of Carrier Concentration at 800 K. Therefore, variations at higher temperatures are more dominant in all of these compounds as compared to lower temperature ranges. Overall, the $CaCr_2As_2$ compound started with a larger value and achieved the second highest magnitude value among four, at about 800 K. The $CaCr_2P_2$ and $SrCr_2As_2$ compounds initially started with the same value at about 50 K and reached their maximum value in higher temperature ranges. The carrier concentration drops a lot when the temperature is lower than 300 K for $SrCr_2As_2$.

4. Summary

In summary, we have performed the electronic, magnetic, and thermoelectric properties of KCr_2L_2 (K= Ca, Sr; L = P, As) using first-principle calculation. We noted that these compounds are more favorable in the antiferromagnetic arrangement as compared to FM and PM configurations. The electronic properties (DOS) show a readable hybridization of *d* (Cr) and *p* (P/As) orbitals in a broad energy range. Besides, for these compounds the total magnetic moment is originated

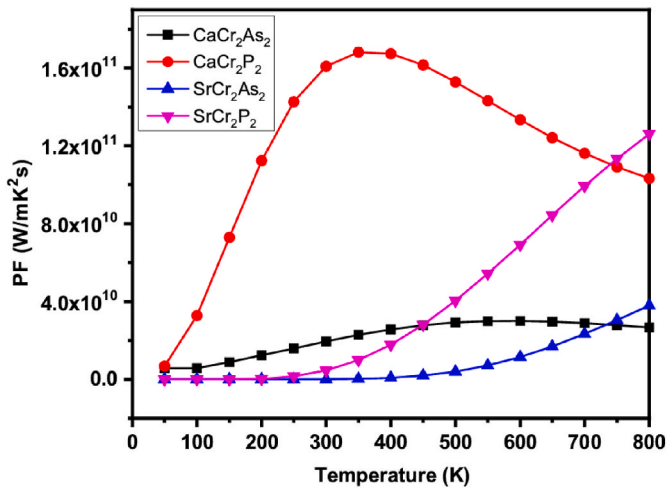

Fig. 8. Thermoelectric power factor ($S^2\sigma/\tau$) versus temperature for KCr_2L_2 (K═Ca, Sr and L = As, P).

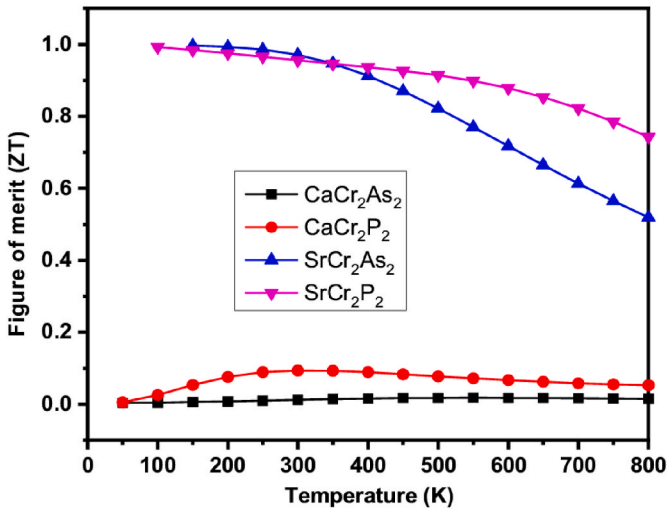

Fig. 9. Temperature-dependent variations of figure of merit (ZT) for KCr_2L_2 (K═Ca, Sr and L = As, P).

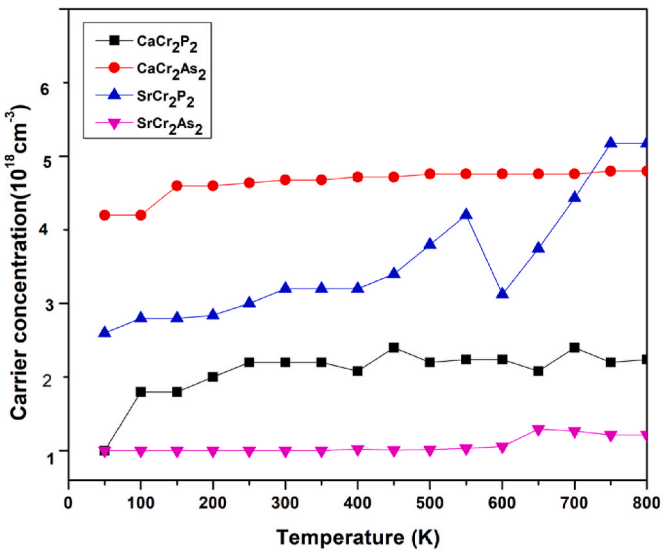

Fig. 10. Temperature-dependent carrier concentration for KCr_2L_2 (K═Ca, Sr and L = As, p).

mostly from Cr magnetic spins ordering that establishes the ferromagnetic behavior. The TDOS are symmetrical which give us positive response in antiferromagnetic case that both (up and down) of magnetic moment are zero. Both the Cr atoms are well coupled antiferromagnetically the AFM phase. Therefore, these materials may be novel candidates for spintronics and magnetic applications. The Seebeck coefficient (S) shows positive values for $CaCr_2As_2$ and $SrCr_2As_2$ over the entire temperature range, exhibiting compounds with p-type nature, while positive values till 350 K for $CaCr_2P_2$ and $SrCr_2P_2$ along with negative obtained values further higher in temperature ranges exhibit mix p-n type conduction behavior. Moreover, the maximum ZT value attains by the compounds are ~1 for $SrCr_2As_2$ and $SrCr_2P_2$. Our prediction reveals, the strontium-based compounds as promising candidates for low temperature applications in waste heat management.

Credit author statement

Zeshan Zada: Methodology, **Abdul Ahad Khan**: Formal analysis, **Ali H. Reshak**: Writing – review & editing, **Irfan khan**: Software, **Shafqat zada**: Validation, **Muhammad Ismail**: Data curation, **Muhammad Fazal-ur-Rehman**: Methodology, **Muhammad Saqib**: Formal analysis, **G. Murtaza**: Methodology, **Qaisar Khan**: Data curation, **Muhammad M. Ramli**: Investigation.

Declaration of competing interest

The authors declare that they have no known competing financial interests or personal relationships that could have appeared to influence the work reported in this paper.

Data availability

No data was used for the research described in the article.

References

[1] G. Pilania, P.V. Balachandran, C. Kim, T. Lookman, Finding new perovskite halides via machine learning, Frontiers in Mat 3 (2016) 19.
[2] E.A. Moore, Computational modelling of inorganic solids, annual reports section, A"(Inorganic Chemistry) 104 (2008) 46–63.
[3] S. A Dar, V. Srivastava, U.K. Sakalle, Ab initio high pressure and temperature investigation on cubic PbMoO3 perovskite, J. Electron. Mater. 46 (12) (2017) 6870–6877.
[4] F. Tran, P. Blaha, Accurate band gaps of semiconductors and insulators with a semilocal exchange-correlation potential, Phy. Rev. Let 102 (22) (2009), 226401.
[5] D.D. Koelling, B.N. Harmon, A technique for relativistic spin-polarised calculations, J. Phys. C Solid State Phys. 10 (16) (1977) 3107.
[6] Z. Zada, A. Laref, G. Murtaza, A. Zeb, A. Yar, First-principles calculations of electronic and magnetic properties of XMn2Y2 (X= Ca, Sr; Y= Sb, Bi) compounds, Int. J. Mod. Phys. B 33 (18) (2019), 1950199.
[7] Z. Zada, H. Ullah, R. Zada, S. Zada, A. Laref, S. Azam, M. Irfan, Structure stability, half metallic ferromagnetism, magneto-electronic and thermoelectric properties of new zintl XCr2Bi2 (X= Ca, Sr) compounds for spintronic and renewable energy applications, Phys. B Condens. Matter 607 (2021), 412866.
[8] A.A. Khan, W. Khan, A. Khan, A. Laref, A. Zeb, G. Murtaza, Investigation of the structural, electrical, optical and magnetic properties of XMg4Mn6O15 (X= K, Rb, and Cs) comp, Mater. Res. Express 6 (6) (2019), 066102.
[9] Z. Zada, H. Ullah, R. Bibi, S. Zada, A. Mahmood, Electronic band profiles and magneto-electronic properties of ternary XCu2P2 (X= Ca, Sr) compounds: insight from ab initio calculations, Z. Naturforsch. 75 (6) (2020) 543–549.
[10] M.I. Katsnelson, V.Y. Irkhin Chioncel, A.I.L. Lichtenstein, R.A. de Groot, Half-metallic ferromagnets: from band structure to many-body effects, Rev. Mod. Phys. 80 (2) (2008) 315.
[11] A. Hirohata, K. Takanashi, Future perspectives for spintronic devices, J. Phys. D Appl. Phys. 47 (19) (2014), 193001.
[12] S.A. Wolf, D.D. Awschalom, R.A. Buhrman, J.M. Daughton, V.S. von Molnár, M. L. Roukes, D.M. Treger, Spintronics: a spin-based electronics vision for the future, Science 294 (5546) (2001) 1488–1495.
[13] J.A. Brug, T.C. Anthony, J.H. Nickel, Magnetic recording head materials, MRS Bull. 21 (9) (1996) 23–27.
[14] S. Bobev, J.D. Thompson, J.L. Sarrao, M.M. Olmstead, H. Hope, S.M. Kauzlarich, Probing the limits of the Zintl concept: structure and bonding in rare-earth and alkaline-earth zinc- antimonides Yb9Zn4+xSb9 and Ca9Zn4.5Sb 9, Inorg. Chem. 43 (16) (2004) 5044–5052.
[15] E. Morosan, H.W. Zandbergen, B.S. Dennis, J.W.G. Bos, Y. Onose, T. Klimczuk, .R. J. Cava, Superconductivity in cuxtise2, Nat. Phys. 2 (8) (2006) 544–550.
[16] G. Li, W.Z. Hu, D. Qian, D. Hsieh, M.Z. Hasan, E. Morosan, .N.L. Wang, Semimetal-to-Semimetal charge density wave transition in 1 T− TiSe2, Phys. Rev. Lett. 99 (2) (2007), 027404.
[17] M.N. Ali, J. Xiong, S. Flynn, J. Tao, Q.D. Gibson, L.M. Schoop, R.J. Cava, Large, non-saturating magnetoresistance in WTe2, Nat 514 (7521) (2014) 205–208.
[18] X.C. Wang, U.Q. Liu, V.Y. Lv, W.B. Gao, L.X. Yang, R.C. Yu, .C.Q. Jin, The superconductivity at 18 K in LiFeAs system, Solid State Commun. 148 (11–12) (2008) 538–540.
[19] M. Rotter, M. Tegel, D. Johrendt, Superconductivity at 38 K in the iron arsenide (Ba 1− x K x) Fe 2 as 2, Phy. Rev. Let 101 (10) (2008), 107006.
[20] F.C. Hsu, J.Y. Luo, K.W. Yeh, T.K. Chen, T.W. Huang, P.M. Wu, M.K. Wu, Superconductivity in the PbO-type structure α-FeSe, Proc. Natl. Acad. Sci. USA 105 (38) (2008) 14262–14264.
[21] H. Schäfer, On the problem of polar intermetallic compounds: the stimulation of E. Zintl's work for the modern chemistry of intermetallics, Annu. Rev. Mater. Sci. 15 (1) (1985) 1–42.
[22] S.M. Kauzlarich, Chemistry, Structure and Bonding of Zintl Phases and Ions, Wiley-VCH, Weinheim, 1996.
[23] H. Schäfer, B. Eisenmann, W. Müller, Zintl-Phasen: Übergangsformen zwischen Metall-und Ionenbindung, Angew. Chem. 85 (17) (1973) 742–760.
[24] G. Murtaza, N. Yousaf, M. Yaseen, A. Laref, S. Azam, Systematic studies of the structural and optoelectronic characteristics of $CaZn_2X_2$ (X= N, P, As, Sb, Bi), Mater. Res. Express 5 (1) (2018), 016304.
[25] A. Mewis, AB2X2-Verbindungen im CaAl2Si2-Typ, V[1] Zur Struktur der Verbindungen CaMn2P2, CaMn2As2, SrMn2P2 und SrMn2As2/AB2X2-Compounds with the CaAl2Si2 Structure, V [1] The Crystal Structure of CaMn2P2, CaMn2As2, SrMn2P2, and SrMn2As2, Z. Naturforsch. B Chem. Sci. 33 (6) (1978) 606–609.
[26] J. Zeng, S. Qin, C. Le, J. Hu, Magnetism and superconductivity in the layered hexagonal transition metal pnictides, Phys. Rev. B 96 (17) (2017), 174506.
[27] S. Calder, B. Saparov, H.B. Cao, J.L. Niedziela, M.D. Lumsden, A.S. Sefat, A. D. Christianson, Magnetic structure and spin excitations in BaMn 2 Bi 2, Phys. Rev. B 89 (6) (2014), 064417.
[28] R. Hoffmann, C. Zheng, Making and breaking bonds in the solid state: the ThCr2Si2 structure, J. Phys. Chem. 89 (20) (2002) 4175–4181.
[29] R. Hoffmann, C. Zheng, in: A. Veillard (Ed.), Quantum Chemistry: the Challenge of Transition Metals and Coordination Chemistry", Reidel, Dordrecht, 1986.
[30] C. Zheng, R. Hoffmann, R. Nesper, H.G. Von Schnering, Site preferences and bond length differences in CaAl2Si2-type Zintl compounds, J. Am. Chem. Soc. 108 (8) (1986) 1876–1884.
[31] C. Zheng, R. Hoffmann, Complementary local and extended views of bonding in the ThCr2Si2 and CaAl2Si2 structures, J. Solid State Chem. 72 (1) (1988) 58–71.
[32] C. Zheng, Bonding and dynamics of the thorium chromium silicide (ThCr2Si2) and calcium beryllium germanide (CaBe2Ge2) type main group solids: a Monte Carlo simulation study, J. Am. Chem. Soc. 115 (3) (1993) 1047–1051.
[33] P. Klüfers, A. Mewis, AB2X2-Verbindungen im CaAl2Si2-Typ, III Zur Struktur der Verbindungen CaZn2P2, CaCd2P2, CaZn2As2 und CaCd2As2/AB2X2 Compounds with the CaAl2Si2 Structure, III The Crystal Structure of CaZn2P2, CaCd2P2, CaZn2As2, and CaCd2As2, Z. Naturforsch. B Chem. Sci. 32 (7) (1977) 753–756.
[34] G. Murtaza, A.A. Khan, M. Yaseen, A. Laref, N. Ullah, I. ur Rahman, The effect of replacing pnictogen elements on the physical properties SrMg2 (, P, As, Sb, Bi) Zintl compounds, Chin. Phys. B 27 (4) (2018), 047102.
[35] A. Mewis, Ternäre Phosphide mit ThCr2Si2-Struktur/Ternary Phosphides with the ThCr2Si2 Struc, Z. Naturforsch. B Chem. Sci. 35 (2) (1980) 141–145.

[36] J.F. Li, W.S. Liu, L.D. Zhao, M. Zhou, High-performance nanostructured thermoelectric materials, NPG Asia Mater. 2 (4) (2010) 152–158.
[37] L.D. Zhao, D. Berardan, Y.L. Pei, C. Byl, L. Pinsard-Gaudart, N. Dragoe, Bi 1− x Sr x CuSeO oxyselenides as promising thermoelectric materials, Appl. Phys. Lett. 97 (9) (2010), 092118.
[38] Junphil Hwang, et al., More than Half Reduction in Price Per Watt of Thermoelectric Device without Increasing the Thermoelectric Figure of Merit of Mat, School of Mechanical Engineering, Yonsei University, Seoul, 2017.
[39] P. Hohenberg, W. Kohn, Inhomogeneous electron gas, Phys. Rev. 136 (1964) B864, https://doi.org/10.1103/PhysRev.136.B864.
[40] W. Kohn, L.J. Sham, Self-consistent equations including exchange and correlation effects, Phys. Rev. 140 (4A) (1965) A1133.
[41] P. Blaha, K. Schwarz, G.K.H. Madsen, D. Kvasnicka, J. Luitz, WIEN2K, An Augmented Plane Wave Plus Local Orbitals Program for Calculating Crystal Properties, Vienna University of Technology, Vienna, 2001.
[42] J.P. Perdew, K. Burke, M. Ernzerhof, Generalized gradient approximation made simple, Phys. Rev. Lett. 77 (1996) 3865, https://doi.org/10.1103/PhysRevLett.77.3865.
[43] H.J. Monkhorst, J.D. Pack, Special points for Brillouin-zone integrations, Phys. Rev. B 13 (12) (1976) 5188.
[44] D. James Pack, J. Hendrik Monkhorst, Special points for Brillouin-zone integrations"—a reply, Phys. Rev. B 16 (4) (1977) 1748.
[45] M. Sahnoun, C. Daul, O. Haas, A. Wokaun, Investigation of the electronic structure in La1− xCaxCoO3 (x= 0, 0.5) using full potential calcul, J. Phys. Condens. Matter 17 (50) (2005) 7995.
[46] X. Du, L. Mihaly, P.B. Allen, Wiedemann-Franz law in Bi2Sr2CaCu2O8, Phys. B Condens. Matter 194 (1994) 1507–1508.
[47] Z. Zada, H. Ullah, R. Zada, A.A. Khan, A. Mahmood, S.M. Ramay, Electronic band profiles, magnetic stability, antiferromagnetic spins ordering and thermodynamics properties of novel antiferromagnet CaCr2Sb2, European Phys. J. Plus 136 (4) (2021) 1–12.
[48] R. Bibi, Z. Zada, A.A. Khan, S. Azam, M. Irfan, B.U. Haq, S.A. Khan, First-principles calculations of structural, electronic, magnetic, thermoelectric, and thermodynamic properties of BaMn2P2 in the Anti and ferromagnetic phase, J. Solid State Chem. (2021), 122388.
[49] Z. Zada, A.A. Khan, A.H. Reshak, M. Ismail, S. Zada, G. Murtaza, J. Bila, Cationic variation for LnAl2Si2 (Ln= Y, Sm, Tb, Dy, Yb) compounds by density functional theory, J. Mol. Struct. 1252 (2022), 132136.
[50] A.A. Khan, Z. Zada, A.H. Reshak, J. Akbar, M. Saqib, M.A. Naeem, M. Ramli, Effects of anion-ligands replacement on the structural, electronic and magnetic properties of ThCo2X2 (X= Si, Ge), Chin. J. Phys. 77 (2022) 956–964.
[51] Z. Zada, A.A. Khan, R. Zada, A.H. Reshak, G. Murtaza, M. Saqib, J. Bila, First-principles calculations to investigate variation of cationic-ligand LmAl2Ge2 (Lm= Ca, Y, La and Ce), Indian J. Phys. (2022) 1–9.
[52] A.A. Khan, M. Yaseen, A. Laref, G. Murtaza, Impact of anion replacement on the optoelectronic and thermoelectric properties of CaMg2X2, X=(N, P, As, Sb, Bi) compounds, Phys. B Condens. Matter 541 (2018) 24–31.
[53] A.A. Khan, M. Saqib, Z. Zada, F. Chahed, M. Ismail, M. Ishaq, M. Faizan, Electronic structure, magnetic, and thermoelectric properties of BaMn2As2 compound: a first-principles study, Phys. Scripta 97 (6) (2022), 065810.
[54] M. Siddique, A. Iqbal, A.U. Rahman, S. Azam, Z. Zada, N. Talat, Mechanical and thermodynamic stability, structural, electronics and magnetic properties of new ternary thorium-phosphide silicides ThSixP1-x: first-principles investigation and prospects for clean nuclear energy applications, Nucl. Eng. Technol. 53 (2) (2021) 592–602.
[55] A.A. Khan, R. Hasil, A. Laref, N. Ullah, M. Sajjad, A. Zeb, G. Murtaza, DFT prediction of the structural, electronic, thermoelectric and optical properties of ternary pnictides MgBe2X2 (X= N, P, As, Sb, Bi): a novel analysis of beryllium with 2A-and 5B-Elements of the structure type CaAl2Si2, Solid State Commun. 300 (2019), 113667.
[56] G. Murtaza, A.A. Khan, M.M. AL-Anazy, A. Laref, Q. Mahmood, Z. Zada, M. Aman, Anionic variations for BaMg2X2 (X= N to Bi) compounds by density functional theory, European Phys. J. Plus 136 (2) (2021) 1–16.
[57] A.A. Khan, A.H. Reshak, Z. Zada, M. Saqib, Z. Abbas, M. Ismail, A. Laref, Thermoelectric, structural, electronic, magnetic, and thermodynamic properties of CaZn2Ge2 compound, European Phys. J. Plus 137 (3) (2022) 1–12.
[58] I. Rahim, S. Azam, B. Gul, A.A. Khan, N. Yousaf, Z. Zada, H.H. Hegazy, Advances in tuning band gap of graphene by potential doping using DFT: a review, Digest J. Nanomater. Biostruct. (DJNB) 16 (3) (2021) 975–988.
[59] Z. Zada, R. Zada, A.A. Khan, M. Saqib, M.F.U. Rehman, M. Ismail, M. Faizan, Investigation of electronic structure, magnetic stability, spin coupling, and thermodynamic properties of novel antiferromagnets XMn2Y2 (X= Ca, Sr; Y= P, As), J. Mol. Struct. 1268 (2022), 133698.